~~CONFIDENTIAL~~
~~RESTRICTED DATA~~
~~Atomic Energy Act - 1954~~

MASTER

Records

SNPO-C

Subcontract NP-1

WANL-TME-2790
April 1971

Westinghouse Astronuclear Laboratory

WESTINGHOUSE ASTRONUCLEAR LABORATORY CONTRIBUTION TO THE THIRTY - SECOND HIGH TEMPERATURE FUELS COMMITTEE MEETING

11,12,13 MAY 1971

(TITLE UNCLASSIFIED)

DISTRIBUTION OF THIS DOCUMENT IS UNLIMITED

~~CONFIDENTIAL~~
~~RESTRICTED DATA~~
~~Atomic Energy Act - 1954~~

DISCLAIMER

17

CO~~NFIDENTIAL~~
R~~ESTRICTED DAT~~A
~~Atomic Energy Act 1954~~

MASTER

WANL-TME-2790
April 1971

Westinghouse Astronuclear Laboratory

SPECIAL REREVIEW
FINAL
DETERMINATION
Class: U

Reviewer KAW
Class. U
Date 4-26-82

WESTINGHOUSE ASTRONUCLEAR LABORATORY CONTRIBUTION TO THE THIRTY - SECOND HIGH TEMPERATURE FUELS COMMITTEE MEETING

11,12,13 MAY 1971

(TITLE UNCLASSIFIED)

Classification cancelled (~~or changed to~~)
by authority of
by H.A.C. TIC, date SEP 1 [illegible]

Prepared By:
L. R. Fleischer

~~GRO - 1~~
~~EXCLUDED FROM AUTOMA WNGRADING~~
~~AND DECL FICATI~~

INFORMATION CATEGORY
~~C-RD~~
R. A. 4-21-71
AUTHORIZED CLASSIFIER DATE

(The preliminary information presented in this report should not be published without prior written approval of the Westinghouse Astronuclear Laboratory. The work performed was supported by the Space Nuclear Propulsion Office).

C~~ONFIDENTIA~~L
R~~ESTRICTED DAT~~A
Ato~~mic Energy Act 1954~~

DISTRIBUTION OF THIS DOCUMENT UNLIMITED

TABLE OF CONTENTS

LIST OF ILLUSTRATIONS

1.0 INTRODUCTION

(U) The successes of the NERVA technology program have led to a steady increase in performance requirements. These have been matched by a steady upgrading of reactor capabilities. From the early tests, the KIWI series and NRX-A2, which demonstrated reactor lifetimes of a few minutes before the fuel came apart, the improvement has been remarkable. NRX-A6 was operated for the planned 60 minutes and still had sufficient reactivity to expect another hour's operation. XE-Prime confirmed these data. In keeping with historical precedent, new, more difficult goals have been set: a multiple restart capability and longer cumulative operating time, 60 operating cycles of 10 minutes duration are desired.

(U) A complete reactor design review was made as a result of the new goals. Many design changes and many materials changes have been specified. After a study in which seven fuel element candidates were evaluated, a carbide/graphite composite fuel concept was selected. The first phases of the plan to develop this fuel are reported in this document. Since corrosion protection mechanisms similar to those used in the graphite based dispersion fuel elements will apply to the composite fuel, the fuel testing and analysis in progress is to be completed. Pre-reactor test performance of PW-2 fuel (graphite base) is also discussed in the following pages.

2.0 PW-2 FUEL PERFORMANCE

(U) The fuel produced for the PW-2 test reactor is generally similar to previous NERVA fuels: a dispersion of coated UC_2 particles in a graphitic matrix with carbide surface coatings. However, modifications have been introduced in the properties of the graphite and in the mechanical interaction between matrix and coating to give satisfactory performance under the new, more stringent, cyclic reactor operating conditions.

(U) The rationale for the changes can be explained by discussion of the correlation of fuel corrosion behavior with "resistance parameter," R_p. Incremental resistance measurements are made on fuel elements at various stages of the fabrication process. An element ready for coating has an essentially uniform value of resistance (on the order of 3.1 mΩ/in.) for each inch of its length. After the coating operation, the fuel element's incremental resistance curve reflects the coating thickness profile as shown in Figure 2.1. If it is assumed that the matrix and the coating act as parallel conductors in the measuring circuit, then the component of the measured resistance, R, attributable to the coating is found from: $\frac{1}{R_{coating}} = \frac{1}{R} - \frac{1}{R_{matrix}}$. If the coating were free of cracks, its resistance would be a function of the coating thickness and the resistivity of the carbide. The difference between this ideal value, R_o, and the experimentally determined $R_{coating}$ is defined as the resistance parameter R_p.

(U) The physical interpretation of R_p depends on the nature of the matrix/coating interface. When the coating is adherent, in continuous intimate contact with the matrix, R_p is a function of the number of cracks in the coating. It reflects the divergence of the current path from the coating, through the matrix, and back to the coating which occurs at cracks. Variation in crack size in adherent coatings is assumed negligible.

(U) For non-adherent coatings, the interpretation is similar except that the effective crack size becomes the distance between points of matrix/coating contact. Thus, R_p becomes a measure of both the number of cracks and the degree of coating non-adherence.

(CRD) Since early in the NERVA fuel development program it has been evident that corrosion at the inlet end (low temperature) and intermediate regions of the fuel elements was predominantly by direct hydrogen attack on the matrix through coating cracks. At the high temperature outlet end the predominant mechanism has been carbon diffusion through the coating to the coolant stream. These generalities still hold, but a new problem has been added by the requirement for cyclic operation: cracks or defects not present in the as-coated fuel develop as a result of mechanical coating/matrix interaction during cycling. This effect has been observed principally in the high intermediate to hot regions (stations 30 to 45).

Note: Ω = ohms

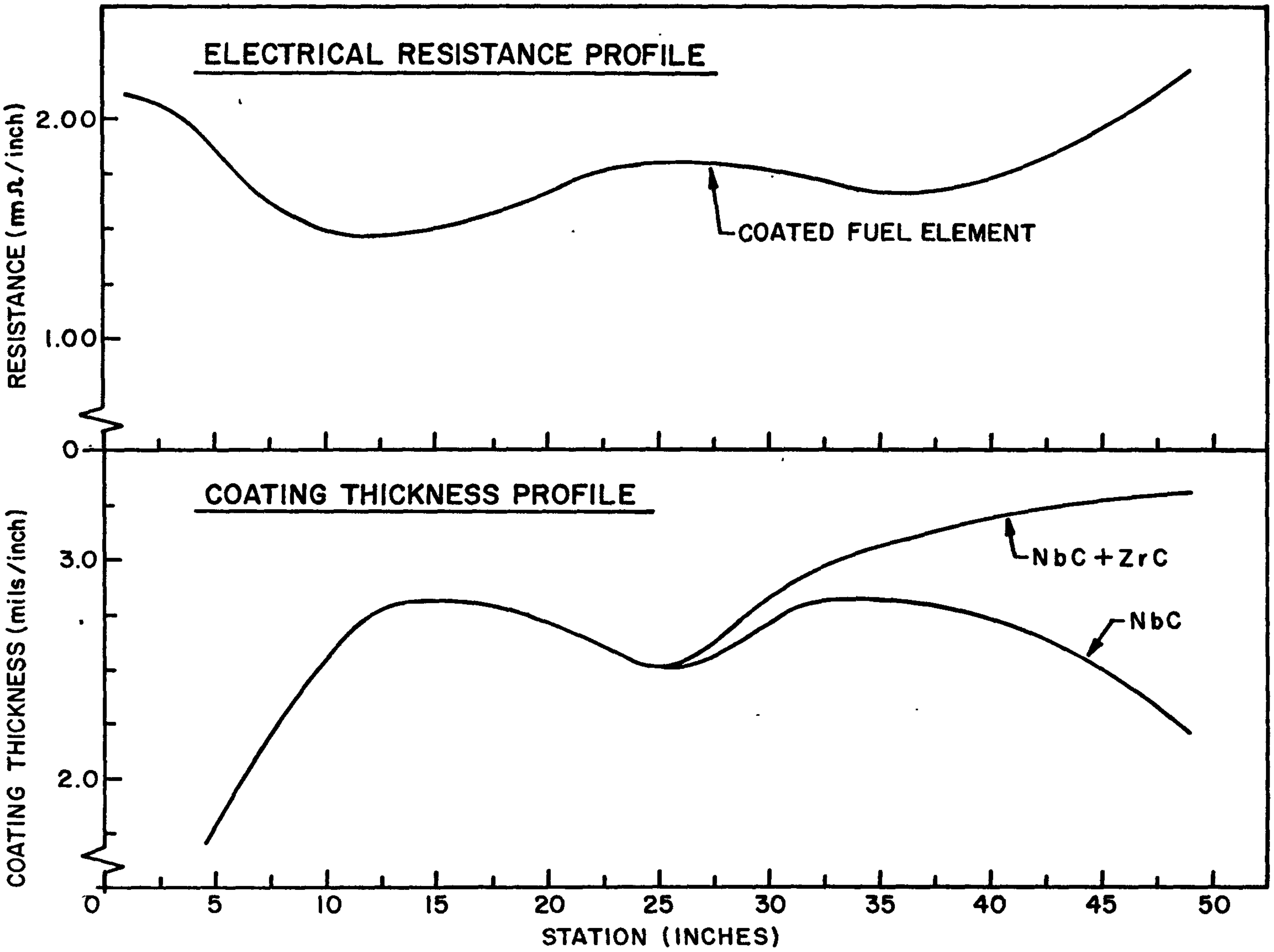

FIGURE 2.1 (U) Electrical Resistance and Coating Thickness Profiles of Typical PW-2 Fuel (C-RD)

(U) Thus, a strategy can be established to minimize corrosion losses. In the low and intermediate temperature regions an adherent coating with a low crack density is desirable. This configuration would be characterized by a low value of R_p. In the region in which "defect" corrosion occurs, the coating should be non-adherent to minimize mechanical interactions, and, thick, diffusion resistant coatings should be used at the hot end. Since the latter two regions overlap, the structure, in practice, must combine non-adherence and diffusion resistance. This structure would be characterized by a relatively high value of R_p.

(CRD) The success of this approach can be seen in the corrosion test data. In six thermal cycles, each including 10 minutes at electrically simulated full power conditions, crack corrosion was minor or absent when R_p values were less than 2 m-ohms/in. in the station 0-35 region; and hot end defect corrosion was inversely related to R_p and tended to be absent when R_p was greater than 4 m-ohms/in. in the hot end. The data illustrating these trends are summarized in Figures 2.2 (station 0-25), 2.3 (stations 25-35), and 2.4 (stations 35-50).

(CRD) The desirable configurations were achieved by the use of high expansion graphites for the matrix. By this means, the CTE of the matrix was brought near to that of the coating minimizing the number of cracks formed in fuel element regions that operate at temperatures below the coating deposition temperature. The initial NbC coating was deposited with carbon provided by methane in the coating gas stream to provide an adherent coating. These techniques provided midband protection adequate to eliminate the need for molybdenum overcoating in the coolant channels.

(CRD) A layer of ZrC was deposited over the initial NbC coating at the hot end (see Figure 2.1). The deposition conditions were such that the carbon was provided by diffusion from the NbC/matrix interface through the NbC. This left a gap between the now non-adherent coating and the matrix in this region.

LEAST SQUARES RELATIONSHIPS BETWEEN MIDBAND CORROSION (A.07 6 x 10) AND R_p FOR FUEL ELEMENTS FROM WANL PW-2 COATING BATCHES

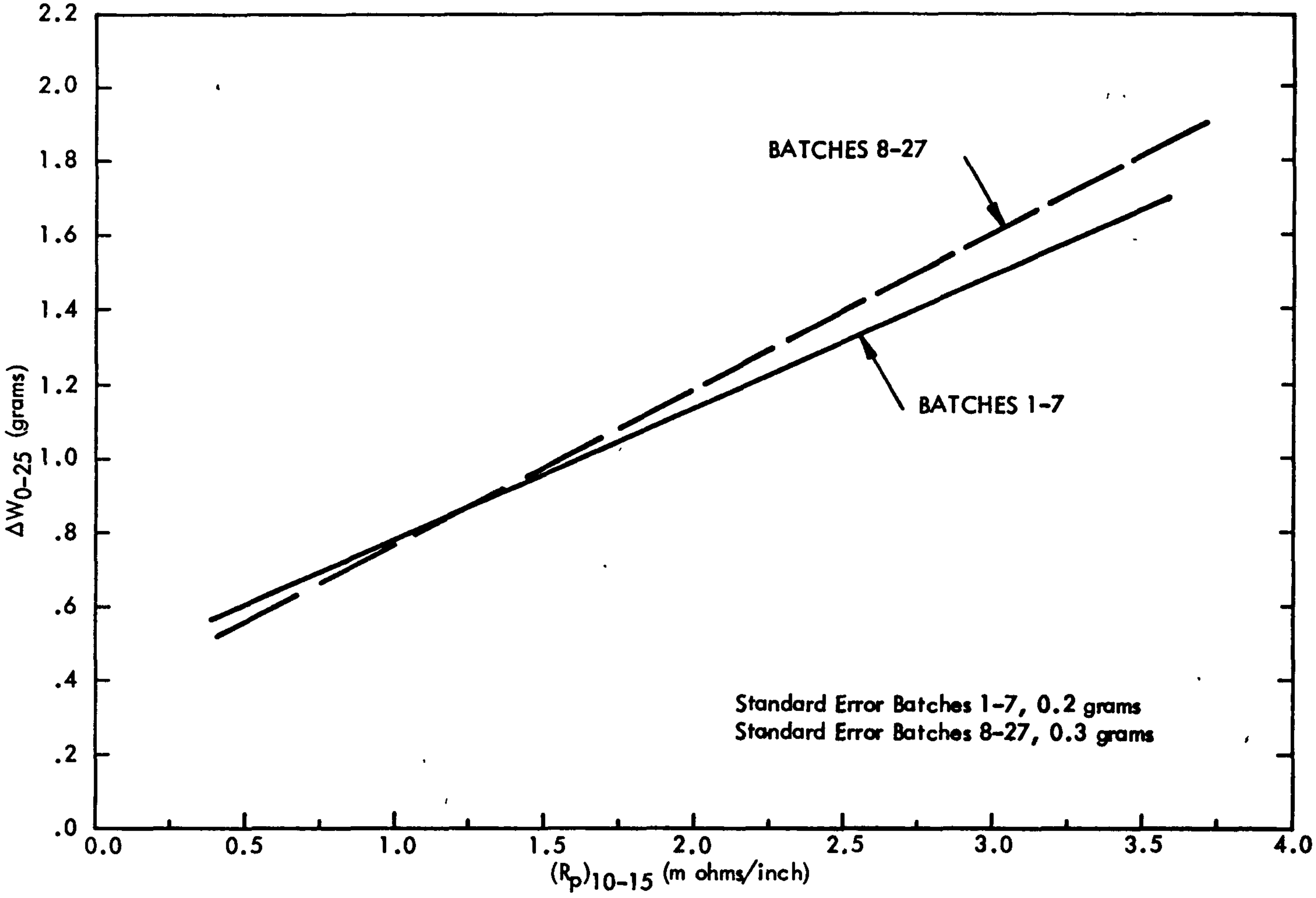

FIGURE 2.2 (U) Least Squares Relationships Between Midband Corrosion (A.07 6 x 10) and R_p for Fuel Elements from WANL PW-2 Coating Batches (C-RD)

LEAST SQUARES RELATIONSHIPS BETWEEN MID ELEMENT CORROSION (A.07 6 x 10) FOR FUEL ELEMENTS FROM WANL PW-2 COATING BATCHES

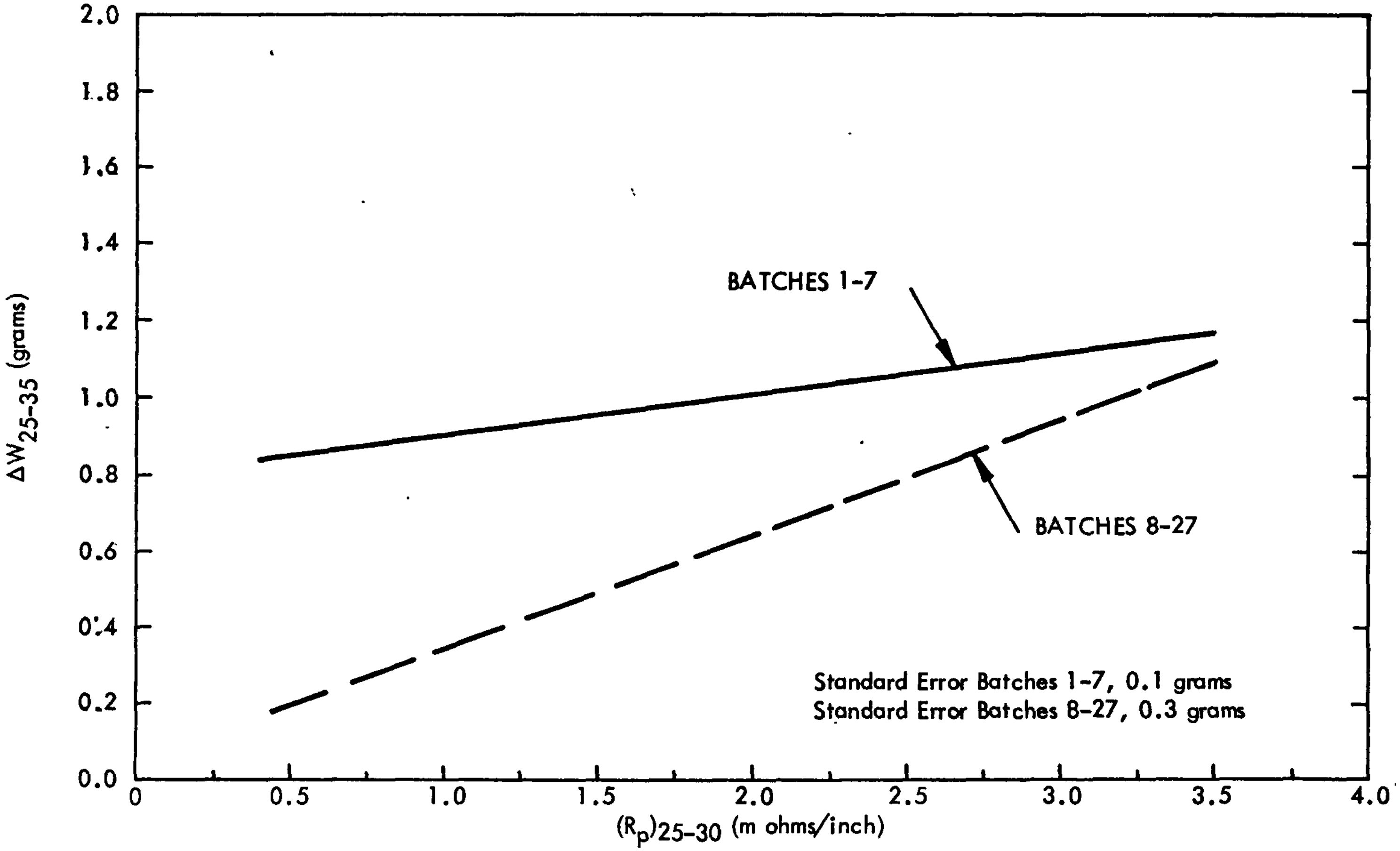

FIGURE 2.3 (U) Least Squares Relationships Between Mid Element Corrosion (A.07 6 x 10) and R_p for Fuel Elements from WANL PW-2 Coating Batches (C-RD)

~~CONFIDENTIAL~~
~~RESTRICTED DATA~~
~~Atomic Energy Act 1954~~

LEAST SQUARES RELATIONSHIPS BETWEEN HOT END CORROSION AND R_p FOR FUEL ELEMENTS FROM WANL PW-2 COATING BATCHES

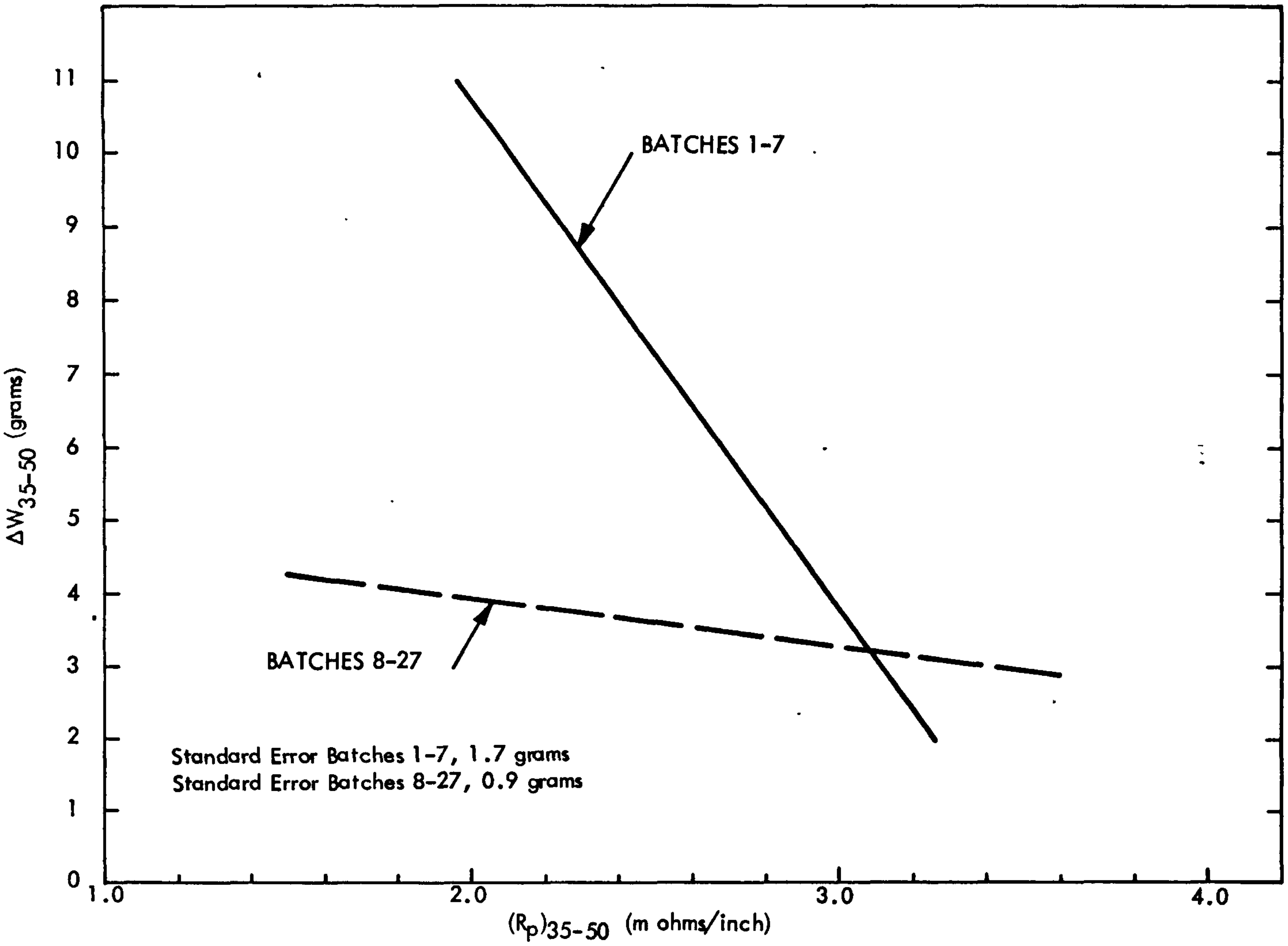

FIGURE 2.4 (U) Least Squares Relationships Between Hot End Corrosion and R_p for Fuel Elements from WANL PW-2 Coating Batches (C-RD)

~~CONFIDENTIAL~~
~~RESTRICTED DATA~~
~~Atomic Energy Act 1954~~

(CRD) The corrosion test data for fuel elements representative of each batch produced for PW-2 is summarized in Figure 2.5. The cross-hatched portion of each bar represents the weight loss of the low to intermediate temperature region of the element (stations 0-35). The clear portion of each bar represents the hot end weight loss. In general, the overall weight losses shown are equivalent to or better than those of the NRX-A6 or XE-Prime reactor fuels reported previously. However, the thermal cycling conditions under which the PW-2 fuel was tested are more severe than those to which previous fuels were subjected even through the total time at temperature is the same.

(CRD) Some elements were tested (under cyclic conditions) for times longer than 60 minutes and showed hot end corrosion rates in the second hour that were 2.5 to 10 times higher than the rates in the first hour. The increased corrosion rates were due to the occurrence of gross defect corrosion in the 30 to 50 inch region which became evident only in the second hour of testing.

(U) The bulk of the fuel of which these tests is representative was used in the assembly of the PW-2 reactor which is now at the Nevada Test Site awaiting test.

3.0 COMPOSITE FUEL DEVELOPMENT

(U) The PW-2 fuel described in the previous section was shown to have inadequate corrosion resistance for operation beyond six 10-minute cycles. With an operational requirement of 60 ten-minute cycles in mind the possibilities for an improved fuel element were surveyed. The decision was made to develop a carbide/graphite composite fuel: a semi-continuous skeleton of (U, Zr)C solid solution carbide in a continuous matrix of graphitic material. These fuel elements are intended to be similar to previous fuels in geometry, the use of carbide protective coatings, and in manufacturing methods, i.e., extrusion.

(U) An initial manufacturing capability has been established based on LASL developed technology. In addition, an extensive program has been initiated to:

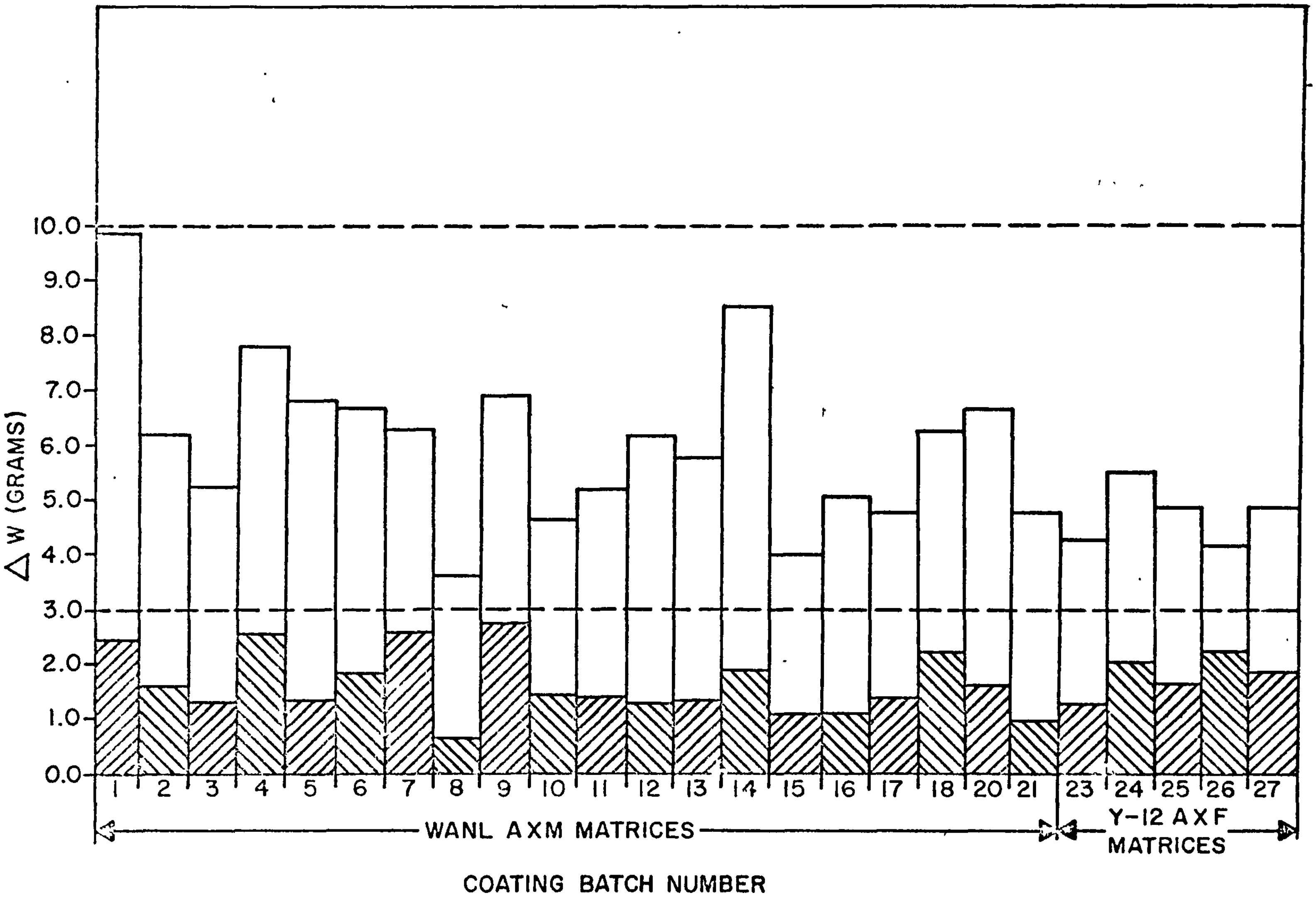

FIGURE 2.5 (U) Q.C. Corrosion Test Behavior of WANL PW-2 Coating Batches (C-RD)

A. Develop and procure advanced raw materials.

B. Develop process parameter/property relationships and define advanced raw materials/process interactions.

The objectives of this program are to improve fuel element thermal stress, to increase fuel element corrosion resistance under cyclic operating conditions, and to provide maximum stability in the solid solution fuel phase.

(U) Changes in all of the raw materials used in fuel element manufacture are under consideration. Graphite flours, lampblacks, and various binders are being developed by the suppliers of these products in conjunction with the project. As with the dispersion fuel elements, the objective is to match the fuel body CTE as closely as possible to that of the protective coating for maximum corrosion protection. However, higher thermal expansion rates can be expected to decrease resistance to thermal stresses. Therefore, increased fuel strength, density, and thermal conductivity, and decreased elastic modulus must compensate.

(U) The current technology introduces the fuel phase as UO_2 and ZrC powders in the extrusion mixture. Carbothermic reaction and diffusion during post-extrusion heat treatment of the fuel elements lead to the formation of the desired solid solution fuel phase. Differences in the properties of the resulting composites have been observed as a function of the sources of the UO_2 and ZrC. However, the most significant effort in this area involves the use of solid solution carbide powder as the starting material. This approach leads to a composite body with a higher carbon density, hence a higher reactivity, permitting substantial reductions in the U concentration. A suitable, single-phase solid solution carbide fuel powder has been developed by a supplier on a subcontract basis.

(U) New vapor deposited coating materials are being developed on subcontract at Battelle Columbus Laboratories. The intent of this work is to reduce carbon losses at the hot ends of fuel elements occurring by diffusion. Carbon diffusion barriers identified by BCL are WC and the nitrides, carbonitrides, and borides of zirconium.

(U) Carbide layer growth data indicate that the carbon diffusion rate in WC may be about 1.5 orders of magnitude lower than in ZrC. In addition to diffusion studies, the compatibilities between various coatings and the fuel matrix, and between coatings and other coatings (since the diffusion barrier may require protection against hydrogen) are under consideration.

(U) The raw materials variations and process parameters are related to fuel materials properties through small tubular extruded samples. This sample configuration was selected to conserve experimental materials available only on a laboratory scale and still allow sufficient numbers of samples to be tested for statistical interpretation of the data. The 1/4 inch O.D. by 1/10 inch I.D. tubular specimens are compatible with a variety of non-destructive and destructive tests used to characterize the fuel materials.

(CRD) Full size fuel elements are also being produced and tested. In corrosion tests, elements made with an intermediate CTE graphite flour (GLC 1074) showed weight losses in 12 ten minute test cycles comparable to the PW-1 fuel element weight losses in 6 ten minute cycles.

(CRD) In addition, the composite fuel elements manufactured from intermediate CTE graphite flour (GLC 1074) showed superior performance to similar elements made from low CTE graphite flour (S-97). The S-97 elements showed a pronounced midband weight loss (at approximately station 10) while the GLC 1074 elements had no midband peak. After a total of 120 minutes of test, the S-97 elements had station 0-25 weight losses of 4 grams versus 0.45 grams for the GLC 1074 elements. The midband weight loss peaks and corresponding microstructures of these element types are compared in Figure 3.1.

(CRD) Metallographically, the corrosion at station 10 in S-97 elements originated at bore coating cracks and was seen as attack on graphite flour particles. Midband corrosion was not metallographically observable in GLC 1074 elements.

(CRD) The hot end weight losses in the two types of element were similar. Metallographic studies showed that these losses occurred through two mechanisms, minor defect corrosion in the 30 to 40 inch region and diffusion corrosion in the 40 to 50 inch region. An additional

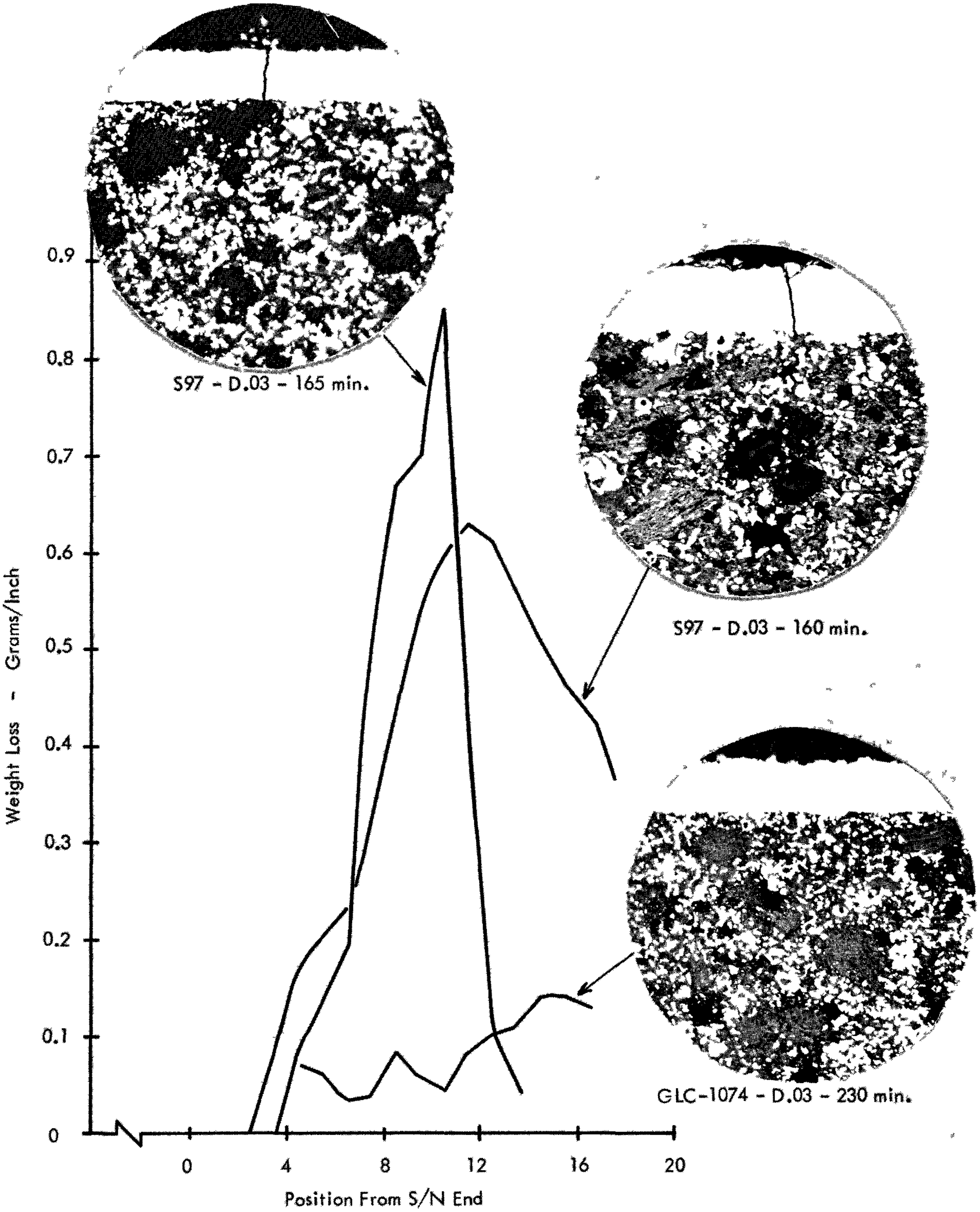

FIGURE 3.1 (U) Comparison ot Midband Corrosion in S-97 and GLC 1074 Elements (C-RD)

contribution to the hot end losses was due to corrosion of the external surfaces of unknown origin. The overall weight loss profiles are compared in Figure 3.2.

~~CONFIDENTIAL~~
~~RESTRICTED DATA~~
~~Atomic Energy Act 1954~~

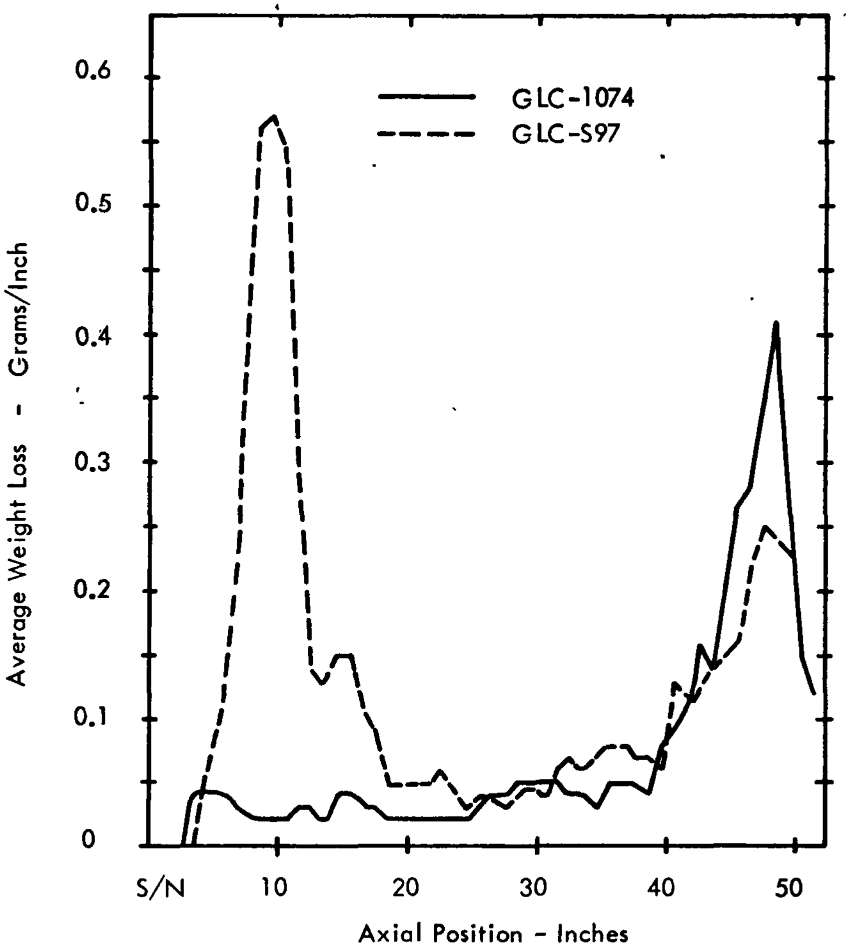

Avg. Weight Loss (Grams)

Position	S97	1074
0-25	3.87	0.59
25-35	0.50	0.42
35-52	2.12	2.81
Total	6.49	3.82

FIGURE 3.2 (U) Typical Weight Loss Profiles for S-97 and GLC 1074 Composite Elements After 120 Minutes Testing (C-RD)

~~CONFIDENTIAL~~
~~RESTRICTED DATA~~
~~Atomic Energy Act 1954~~